Aging predisposes to acute inflammatory induced pathology after tumor immunotherapy

Myriam N. Bouchlaka,[1] Gail D. Sckisel,[3] Mingyi Chen,[4] Annie Mirsoian,[3] Anthony E. Zamora,[3] Emanual Maverakis,[7] Danice E.C. Wilkins,[1] Kory L. Alderson,[1] Hui-Hua Hsiao,[3] Jonathan M. Weiss,[8] Arta M. Monjazeb,[5] Charles Hesdorffer,[9] Luigi Ferrucci,[9] Dan L. Longo,[10] Bruce R. Blazar,[11] Robert H. Wiltrout,[8] Doug Redelman,[2] Dennis D. Taub,[10] and William J. Murphy[3,6]

[1]Department of Microbiology & Immunology and [2]Department of Physiology and Cell Biology, University of Nevada-Reno School of Medicine, Reno, NV 89557
[3]Department of Dermatology, [4]Department of Pathology & Laboratory Medicine, [5]Department of Radiation Oncology, and [6]Department of Internal Medicine, University of California, Davis, Davis, CA 95817
[7]VA Northern California Health Care System, Mather, CA 95655
[8]Cancer and Inflammation Program, National Cancer Institute, Frederick, MD 21702
[9]Clinical Research Branch and [10]Laboratory of Immunology, National Institute on Aging, Baltimore, MD 21224
[11]Division of Blood and Marrow Transplantation, Department of Pediatrics, University of Minnesota, Minneapolis, MN 55455

Cancer commonly occurs in the elderly and immunotherapy (IT) is being increasingly applied to this population. However, the majority of preclinical mouse tumor models assessing potential efficacy and toxicities of therapeutics use young mice. We assessed the impact of age on responses to systemic immune stimulation. In contrast to young mice, systemic cancer IT regimens or LPS given to aged mice resulted in rapid and lethal toxicities affecting multiple organs correlating with heightened proinflammatory cytokines systemically and within the parenchymal tissues. This inflammatory response and increased morbidity with age was independent of T cells or NK cells. However, prior in vivo depletion of macrophages in aged mice resulted in lesser cytokine levels, increased survival, and decreased liver histopathology. Furthermore, macrophages from aged mice and normal human elderly volunteers displayed heightened TNF and IL-6 production upon in vitro stimulation. Treatment of both TNF knockout mice and in vivo TNF blockade in aged mice resulted in significant increases in survival and lessened pathology. Importantly, TNF blockade in tumor-bearing, aged mice receiving IT displayed significant anti-tumor effects. These data demonstrate the critical role of macrophages in the age-associated hyper-inflammatory cytokine responses to systemic immunostimulation and underscore the importance of performing preclinical assessments in aged mice.

CORRESPONDENCE
William J. Murphy:
wmjmurphy@ucdavis.edu

Abbreviations used: ALT, alanine aminotransferase; BMDM, BM-derived macrophage; GVHD, graft-versus-host disease; IT, immunotherapy; LC, liposomal clodronate.

During normal aging, there are significant alterations in immune functions and tissue responses to stimuli. Aging is associated with a low-grade proinflammatory state and a diminished capacity to mount specific adaptive immune responses resulting in susceptibility to pathology after infectious episodes (Boparai and Korc-Grodzicki, 2011). Immunotherapy (IT) in the treatment of cancer has recently resulted in significant clinical responses and is being increasingly applied (Dougan and Dranoff, 2009). However, as cancer also predominantly occurs within the elderly population (Repetto and Balducci, 2002), these immune alterations that occur with aging potentially also render cancer patients more likely to be susceptible to systemic toxicities after application of systemic IT or in response to infection (Repetto and Balducci, 2002; Brüünsgaard and Pedersen, 2003; Ferrucci et al., 2005; Franceschi, 2007; Chung et al., 2009). Elevated serum levels of proinflammatory cytokines, such as IL-1α, IL-1β, IL-6, and TNF, have been observed with increasing age and are believed to be due to an age-related redox imbalance that activates multiple proinflammatory

D.D. Taub and W.J. Murphy contributed equally to this paper.

The Rockefeller University Press $30.00
J. Exp. Med. 2013 Vol. 210 No. 11 2223-2237
www.jem.org/cgi/doi/10.1084/jem.20131219

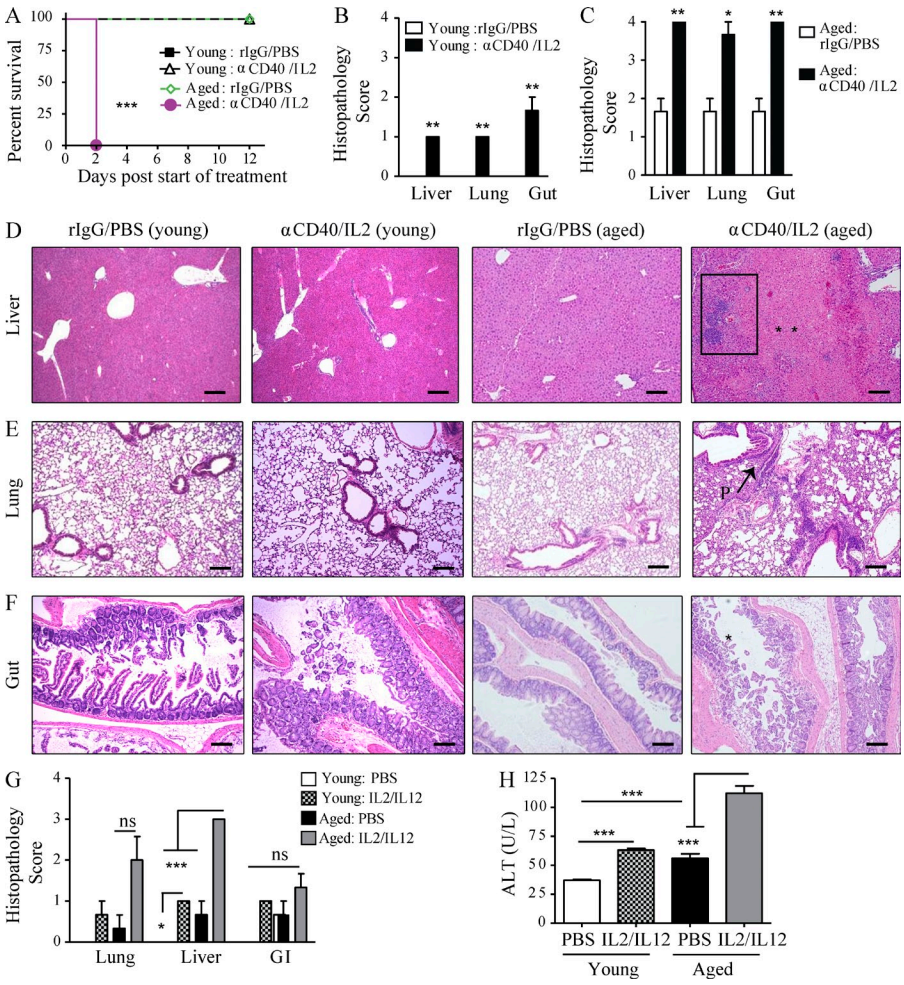

Figure 1. Increased mortality and multiorgan pathology in aged mice after high-dose anti-CD40/IL-2 treatment or after IL-2/IL-12. (A) Survival of young (4 mo) and aged (22 mo) naive C57BL/6 mice that received high-dose anti-CD40/IL-2 or rIgG/PBS, $n = 5–8$. (B–F) Three mice from each treated group in A were evaluated for histopathological differences in the liver at day 2. (B and C) Liver histopathology scoring (see Materials and methods) of young (B) and aged (C) mice. (D–F) Representative images of liver, lung, or gut H&E staining for young or aged mice. Bars, 500 µm. Liver necrosis (D) is indicated by ** and the rectangular area illustrating periportal lymphocytic aggregates. P: peribronchitis (E) in the lungs of aged mice. Gut mucosal erosion and damage (D) in aged mice is indicated by *. Data are representative of one of three independent experiments with similar results. Survival analysis was plotted according to the Kaplan-Meier method, and statistical differences were determined with the log-rank test. ***, $P < 0.001$; **, $P < 0.01$; *, $P < 0.05$. Ctrl: control. (G and H) Young (4 mo) and aged (17 mo) BALB/c mice received either PBS in the control group or 3×10^5 IU IL-2 and 0.5 µg IL-12. (G) Histopathology of the lungs, livers, and gastrointestinal tracts collected at day 11 of treatment were scored and (H) serum ALT was quantified, $n = 3$. Values represent the mean ± SEM of one experiment. Bar graph (mean ± SEM) statistics were determined using two-way ANOVA with Bonferroni's post-test, ***, $P < 0.001$; **, $P < 0.01$; *, $P < 0.05$. n.s.: not significant. &: $P < 0.001$ against all groups. A–F are representative of four and G and H of two independent experiments.

signaling pathways (Franceschi et al., 2000; Brüünsgaard and Pedersen, 2003; Ferrucci et al., 2005; Chung et al., 2009). The mechanisms underlying the causes and contributors to the age-related proinflammatory state remain unclear. Of concern is that the majority of preclinical studies assessing potential immunotherapeutic regimens use younger mice, which likely fail to replicate human clinical cancer treatment conditions with regard to age. Therefore, understanding the impact of age on IT responses and outcome is critical as significant toxicities can be observed with systemic IT (McInnes et al., 1997; Suntharalingam et al., 2006; Waldmann, 2006; Berger et al., 2009; Attarwala, 2010; Di Giacomo et al., 2010; Weber et al., 2012).

Our studies demonstrate that as opposed to young mice, applying systemic IT in aged mice resulted in rapid and lethal responses due to the induction of a proinflammatory cytokine storm and multiorgan pathology. The elevated cytokine responses occurred with numerous immunostimulatory regimens with proinflammatory cytokine production being mediated by macrophages. TNF was a critical mediator for the increased morbidity, as TNF blockade resulted in partial protection from these lethal systemic toxicities and pathology. Application of TNF blockade also led to successful administration of IT while preserving anti-tumor responses in aged mice. These data indicate that aging results in a heightened predisposition to inflammatory responses by macrophages, which leads to increased susceptibility to multiorgan pathology upon challenge.

RESULTS

Anti-CD40 and IL-2 IT results in markedly increased mortality and multiorgan pathology in aged but not young mice

We have previously shown the IT regimen using an agonist anti-CD40 monoclonal antibody in combination with IL-2 to synergize and induce complete regression of metastatic renal cancer in young mice (2–3 mo old; Murphy et al., 2003). As this is roughly equivalent to treating teenage to college-age individuals, we wanted to ascertain whether this IT regimen can be applied to the human cancer scenario with regard to age, so we investigated whether this IT regimen was efficacious

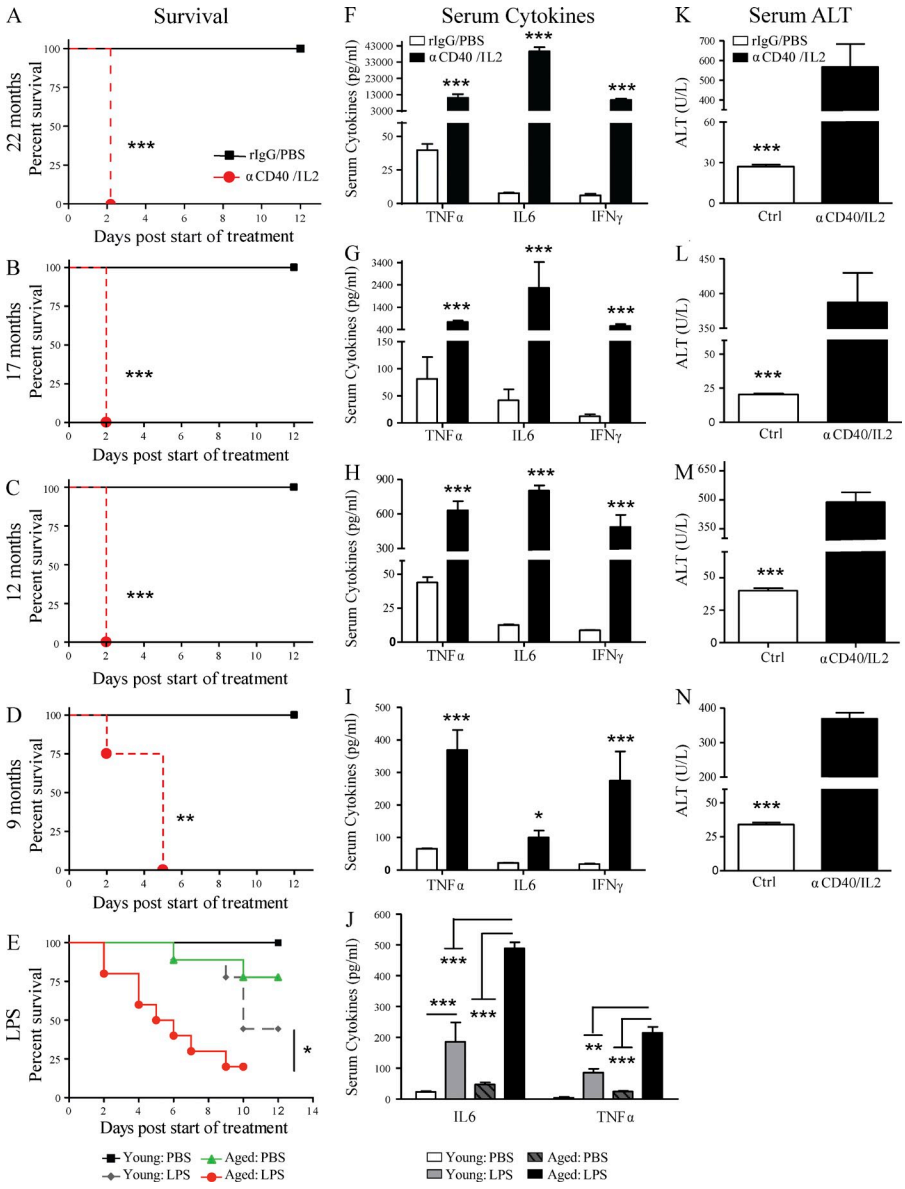

Figure 2. Anti-CD40/IL-2 and LPS-mediated mortality and associated toxicities worsen with age. Survival of aged (A and B; 22 and 17 mo) and middle-aged (C and D; 9 and 12 mo) C57BL/6 mice after high-dose anti-CD40/IL-2 treatment or rIgG/PBS treatment (control). $n = 5$ in controls and $n = 6–8$ in anti-CD40/IL-2. (E) Survival of young (2–4 mo) or aged (17–18 mo) BALB/c mice that received 1.5 mg/kg LPS or PBS on day 0, $n = 9–10$. (F–I) Serum collected from mice of the same age and treatment regimen as in A–D was quantified for TNF, IL-6, and IFN-γ levels. (J) Serum IL-6 and TNF was assessed in young (4 mo) or aged (17–18 mo) mice from 48 h (E) after in vivo PBS or LPS treatment. (K–N) Serum ALT levels (measure of liver necrosis) from mice of F–I. A–D, F–I, and K–N are representative of four independent experiments, and E and J are representative of three independent experiments. Survival analysis was plotted according to the Kaplan-Meier method, and statistical differences were determined with the log-rank test. Bar graph (mean ± SEM) statistics were determined by two-way ANOVA with Bonferroni's post-tests. ***, $P < 0.001$; **, $P < 0.01$; *, $P < 0.05$. Ctrl: control.

in induction of anti-tumor effects in aged tumor-bearing recipients. However, when we treated aged (>16 mo of age) tumor-bearing mice, all the mice rapidly succumbed to the IT within 2 days of regimen administration (unpublished data). To further investigate the IT-induced toxicities with age, we assessed the effects of IT in nontumor-bearing aged mice with anti-CD40/IL-2 IT to ascertain if this rapid mortality was intrinsically related to the age of the recipients. As before, this regimen resulted in a marked and rapid lethality within 2 d of treatment (Fig. 1 A), whereas no mortality was observed in young adult mice.

Necropsy of the aged recipients indicated multiorgan pathologies in response to IT. Aged mice developed marked histopathological changes to the liver (Fig. 1 D), lungs (Fig. 1 E), and gastrointestinal tract (Fig. 1 F) shortly after IT with periportal lymphocytic aggregates in the liver (Fig. 1 D), peribronchiolitis in the lung (Fig. 1 E), and intramucosal lymphocytic aggregates in the gut (Fig. 1 F) compared with their young counterparts. The livers of aged IT-treated mice demonstrated extensive patchy piecemeal necrosis throughout the entire liver (Fig. 1 D). Intestines of aged treated mice showed chronic acute segmental enteritis with extensive mucosal damage, loss of normal villi, and ulceration associated with acute cryptitis (Fig. 1 F). Interestingly, untreated aged mice revealed a preexisting state of mild inflammation even before IT (Fig. 1 C) that was not present in young mice (Fig. 1 B).

We also assessed the effects of other IT regimens. Comparable age-related effects on pathology and serum alanine aminotransferase (ALT) were also observed when aged mice were treated with an IL-2/IL-12 IT regimen (Fig.1, G and H), previously demonstrated to induce potent anti-tumor effects in young mice (Wigginton et al., 1996, 2001). These data indicate that the dramatic induction of a cytokine storm, resulting

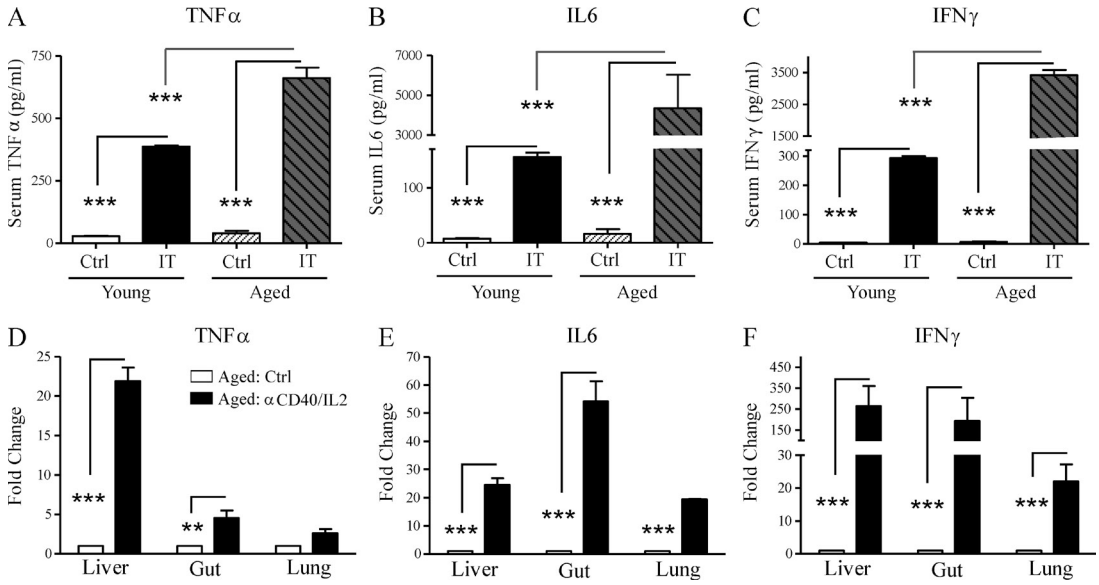

Figure 3. Exacerbated systemic and in situ proinflammatory cytokine production after anti-CD40/IL-2 in aged mice. (A–C) Serum cytokines from young (2 mo) and aged (9 mo) C57BL/6 mice ($n = 3$) that received high-dose anti-CD40/IL-2 (IT) or rIgG/PBS (Ctrl) were measured for TNF, IL-6, and IFN-γ production 48 h after treatment. (D–F) TNF (D), IL-6 (E), and IFN-γ (F) mRNA expression in livers, gut, and lungs of middle-aged (9 mo) treated C57BL/6 mice (day 2), $n = 3$. Data are representative of three independent experiments. Values represent the mean ± SEM of one experiment. Bar graph (mean ± SEM) statistics were determined using two-way ANOVA with Bonferroni's post-test. ***, $P < 0.001$; **, $P < 0.01$ against all groups. Ctrl: control. IT: anti-CD40/IL-2.

in multiorgan pathology and correlating with age after systemic immune stimulation, span a variety of regimens.

Systemic cancer IT or LPS results in increased proinflammatory cytokines and liver enzymes in aged mice

We then delineated as to when the mice developed this sensitivity to IT. Using aged (>16 mo old) mice, anti-CD40/IL-2 IT resulted in a marked and rapid lethality within 2 days of treatment (Fig. 2, A and B). Significantly increased mortality from anti-CD40/IL-2 was also observed in mice as young as 9 mo (middle-aged; Fig. 2, C and D). However, 6-mo-old mice treated with the same regimen of anti-CD40/IL-2 survived the entire IT regimen, indicating that this was the cutoff for the heightened sensitivity (unpublished data). We have also observed similar results in survival, cytokine production, and pathology in aged BALB/c mice comparable to C57BL/6 data presented in Figs. 1 and 2, suggesting that IT-induced toxicities and mortality were strain independent (not depicted).

Mortality from anti-CD40 and IL-2 was only observed after combination therapy, as mice receiving either agent singly survived the full IT regimen. IL-2 and anti-CD40 monotherapy led to an increase in serum IFN-γ and TNF, respectively, compared with the control group; however, these cytokine levels were 7-fold lower for IFN-γ and 50-fold lower for TNF than the combination of anti-CD40/IL-2 (not depicted).

This increased pathological response to IT was not limited to the anti-CD40 and IL-2 regimen. In addition to this IT, aged mice treated with LPS, to mimic a systemic infection (Munford, 2006), yielded similar heightened pathology as they also succumbed to LPS toxicity more rapidly (Fig. 2 E) than young mice. These data demonstrate that strong systemic immune stimulation results in a lethal reaction that correlates with increased age.

The multiorgan pathology (Fig. 1) and increased mortality (Fig. 2, A–D) in aged mice that received anti-CD40/IL-2 IT correlated with markedly increased serum levels of the proinflammatory cytokines TNF, IL-6, and IFN-γ (Fig. 2, F–I). The levels of TNF, IL-6, and IFN-γ after IT also directly correlated with increasing age (Fig. 2, F–I). This cytokine storm associated with aging was not limited to IT, aged mice treated with LPS not only succumbed to LPS toxicity more rapidly (Fig. 2 E) but also demonstrated higher serum levels of TNF and IL-6 compared with younger mice (Fig. 2 J). Heightened serum levels of ALT, indicative of liver damage, were observed in both treated aged (Fig. 2, K and L) and middle-aged (Fig. 2, M and N) mice.

We then compared the inflammatory cytokine levels both in the serum in and in the tissues. IT with anti-CD40/IL-2 resulted in marked increases in both the serum protein (Fig. 3, A–C) and mRNA levels (Fig. 3, D–F) of TNF, IL-6, and IFN-γ within the tissues of the liver, gut, and lungs compared with younger mice. Increase in TNF expression was the highest in the livers of aged mice, whereas IL-6 expression was most increased in the gut and IFN-γ was elevated in all three organs, suggesting that different proinflammatory cytokines may play a more predominant role in a particular organ system. These results demonstrate that the IT-induced mortality and pathology in aged but not young mice is associated with marked induction of proinflammatory cytokines affecting multiple organs correlating with the increased lethality.

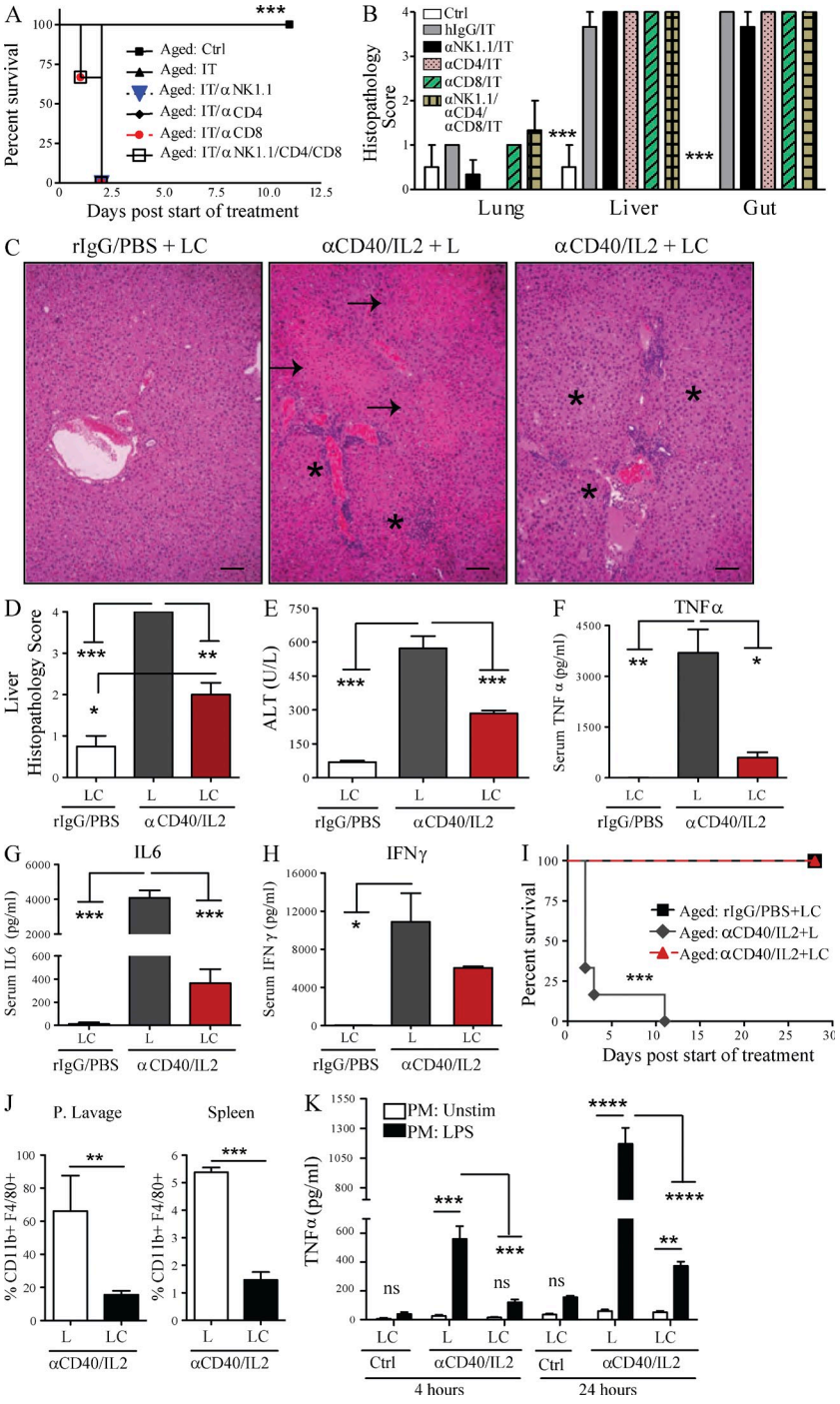

Figure 4. Liver pathology, systemic toxicities, and mortality from anti-CD40/IL-2 in aged mice are macrophage dependent. (A) Survival of aged (9 mo) C57BL/6 after low-dose anti-CD40/IL-2 (IT). At day −3, certain groups were NK depleted (300 µg), CD4 T cell depleted (500 µg), CD8 T cell depleted (500 µg), or received all three depletions before the start (day −3) of anti-CD40/IL-2 (n = 3–4). The control (Ctrl) group received rIgG/PBS. Survival analysis was plotted according to the Kaplan-Meier method, and statistical differences were determined with the log-rank test. (B) Similar treatments as in A were established, and 2 d after the start of IT, mice were euthanized, liver, lung, and intestines were H&E stained, and the histopathology in each organ and group was scored, n = 3. (C–H) Aged (13 mo) C57BL/6 mice received rIgG/PBS or low-dose anti-CD40/IL-2 in combination with liposome clodronate or anti-CD40/IL-2 with liposomes (L) only and euthanized at day 2. (C) Representative images of liver H&E sections. Bars, 500 µm. Asterisks point at lymphocytic infiltrates and arrows represent necrosis. (D and E) Liver histopathology score (D) and serum ALT (E) in all three groups. (F–H) Serum level of TNF (F), IL-6 (G), and IFN-γ (H). (I) Percent survival in aged (13 mo) mice treated with rIgG/PBS + LC, or anti-CD40/IL-2 + L or anti-CD40/IL-2 + LC, n = 6. (J) Percentage of CD11b$^+$ F4/80$^+$ macrophages gated on CD45$^+$ CD19$^-$ in peritoneal lavage or spleen cells from C–H to check for macrophage depletion in anti-CD40/IL-2 + L or anti-CD40/IL-2 + LC groups at day 2, n = 3. (K) Peritoneal lavage cells from mice in C–H were cultured and stimulated with PBS or LPS (50 ng/ml) and TNF levels were measured at 4 and 24 h after treatment. One-way or two-way ANOVA of analysis with Bonferroni's post-tests was performed. Survival analysis was plotted according to the Kaplan-Meier method, and statistical differences were determined with the log-rank test. Values represent the mean ± SEM with Bonferroni's post-test. ***, P < 0.001; **, P < 0.01; *, P < 0.05. n.s: not significant. A–K are representative of three independent experiments.

Macrophages mediate the cytokine storm and mortality in aged mice

We have previously demonstrated that the anti-tumor effects of anti-CD40/IL-2 IT were mediated by marked expansion and activation of CD8 T cells, although NK cells also expanded after treatment (Murphy et al., 2003). CD8 T cells have also been shown to be the principal anti-tumor mediators of IL-2/IL-12 regimens (Wigginton et al., 2001). To determine the immune cells responsible for the toxicities occurring in aged mice after IT, aged mice were first depleted of T cells (using anti-CD4 and anti-CD8 mAbs), NK cells (using anti-NK1.1), or macrophages (with prior treatment with liposomal clodronate [LC]) followed by anti-CD40/IL-2. The absence of CD4 and/or CD8 T cells or NK cells in aged mice all resulted in comparable IT-induced mortality, organ damage (Fig. 4, A and B), and cytokine induction (not depicted). However, macrophage depletion in aged mice resulted in significant and marked protection from IT-induced toxicities. Interestingly, improvement of pathology was primarily observed in the liver (Fig. 4, C and D) and not in the other organs, indicating

that liver pathology was pivotal for the rapid mortality due to the cytokine storm. Macrophage depletion by LC in aged mice was also accompanied by a significant decrease in serum ALT (Fig. 4 E) and proinflammatory cytokines (TNF, IL-6, and IFN-γ; Fig. 4, F–H), and resulted in 100% survival after IT (Fig. 4 I). Depletion of peripheral macrophages was ascertained by flow cytometry (Fig. 4 J). Peritoneal lavage cells recovered from aged mice that were also macrophage-depleted demonstrated significantly lower TNF production upon LPS stimulation, which further demonstrated macrophages as the primary source of proinflammatory cytokines (Fig. 4 K). These data indicate that macrophages, and not lymphocytes, are the major cell type responsible for the IT-related toxicities in aged mice, and that the liver was the principal target organ responsible for mortality.

Murine and human macrophages ex vivo–stimulated with LPS show an age-dependent increase in proinflammatory cytokine production

To further examine the impact of age on the extent of cytokine production by macrophages, BM-derived macrophages (BMDMs) from young and aged mice were isolated and stimulated with LPS. Macrophages from aged mice produced significantly higher TNF and IL-6 compared with young mice (Fig. 5 A). Similarly, human PBMCs, derived from 37 healthy donors ranging from 28 to 95 years old which were differentiated into macrophages in vitro (Zhang et al., 2008) and then stimulated with LPS, revealed a striking age-dependent increase in their ability to produce TNF (Fig. 5, B and D) and IL-6 (Fig. 5, C and E), suggesting that aging (or variables associated with aging) contributes to the increased proinflammatory status of macrophages. The data further suggest that targeting of macrophages may be a potential therapeutic option for systemic immune stimulation, either induced by cancer therapies or during acute sepsis, particularly in the elderly.

TNF-dependent liver toxicity in aged mice after IT

Given the strong correlation of proinflammatory cytokine levels with pathology in the aged mice, we next sought to examine their role in the age-dependent toxicities observed after IT. Macrophage depletion, which allowed for protection from acute organ failure and lethality in the aged, led to significant decreases in TNF and IL-6 expression in particular. Pathological TNF and IL-6 expression has been implicated in various systemic inflammatory conditions (Hack et al., 1989; Gantner et al., 1995; Leon et al., 1998; Taylor and Feldmann, 2009; Krüttgen and Rose-John, 2012). We focused on TNF in these next studies as opposed to other elevated cytokines because of its involvement in a variety of systemic pathological conditions, as well as its pleiotropic effects on other cytokines including IL-6 and IFN-γ, which have been shown to be elevated after IT as well (Boccoli et al., 1990; Blay et al., 1992; Vonderheide et al., 2007). Furthermore, TNF is known to amplify IL-6 production (Shalaby et al., 1989; Sheron et al., 1990; Aggarwal, 2003); therefore, we reasoned that TNF inhibition might account for reductions in other inflammatory

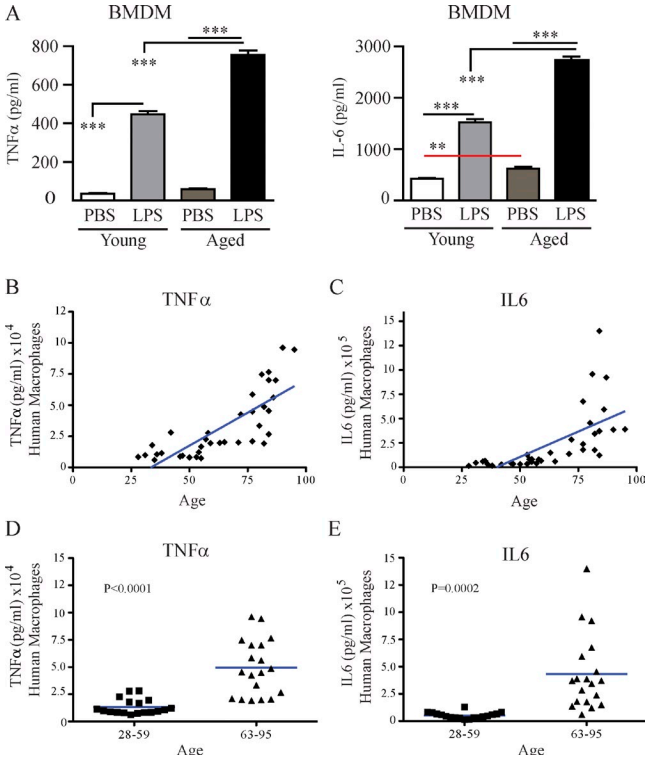

Figure 5. Ex vivo LPS-stimulated mouse and human macrophages have increased TNF and IL-6 production in an age-dependent manner. (A) Young (4 mo) or aged (17–18 mo) C57BL/6 mice received PBS or LPS and on day 3, monocytes from the BM were isolated, differentiated into macrophages (BMDM), and ex vivo restimulated with either PBS or LPS for 24 h to assess TNF and IL-6 levels. (B–E) Monocytes derived from the PBMCs of 37 donors aging from 28 to 95 yr old were isolated and differentiated into macrophages over 10 d and were then stimulated for 48 h with 50 ng/ml LPS or PBS, and TNF and IL-6 production was assessed. Data are illustrated in two different manners: (B and C) data for TNF and IL-6 production by macrophages in donor cohorts ranging from 28 to 59 yr old as a scatter plot; (D and E) data analyzed by grouping the 28–59 and the 63–95 yr olds. Mouse data were analyzed by one-way analysis with Bonferroni's post-tests, $n = 3$. A is representative three independent experiments and B–E are representative of one experiment. Human data in D and E were analyzed by a Student's *t* test (horizontal bars represent means), and p-values are indicated on graphs in C and D.

cytokines. To test this hypothesis, we treated aged WT and aged TNF KO, as well as aged IFN receptor (IFNR)–KO mice with IT, and observed that aged TNF-KO mice were able to survive the entire IT regimen (Fig. 6 A), whereas 50% of the IFNR-KO mice succumbed to IT by day 12 of anti-CD40/IL-2 administration (Fig. 6 A). This indicated a partial involvement of the IFN-γ pathway in toxicities of anti-CD40/IL-2, but that lethality in the aged is predominately dependent on TNF. Aged TNF-KO mice also demonstrated diminished serum levels of IL-6 (Fig. 6 B) as well as the expected lack of TNF (Fig. 6 C), indicating that TNF was at least partially responsible for inducing IL-6 in the cytokine storm. Interestingly, serum IFN-γ levels were increased in aged TNF-KO mice compared with aged WT mice (Fig. 6 D), whereas serum ALT

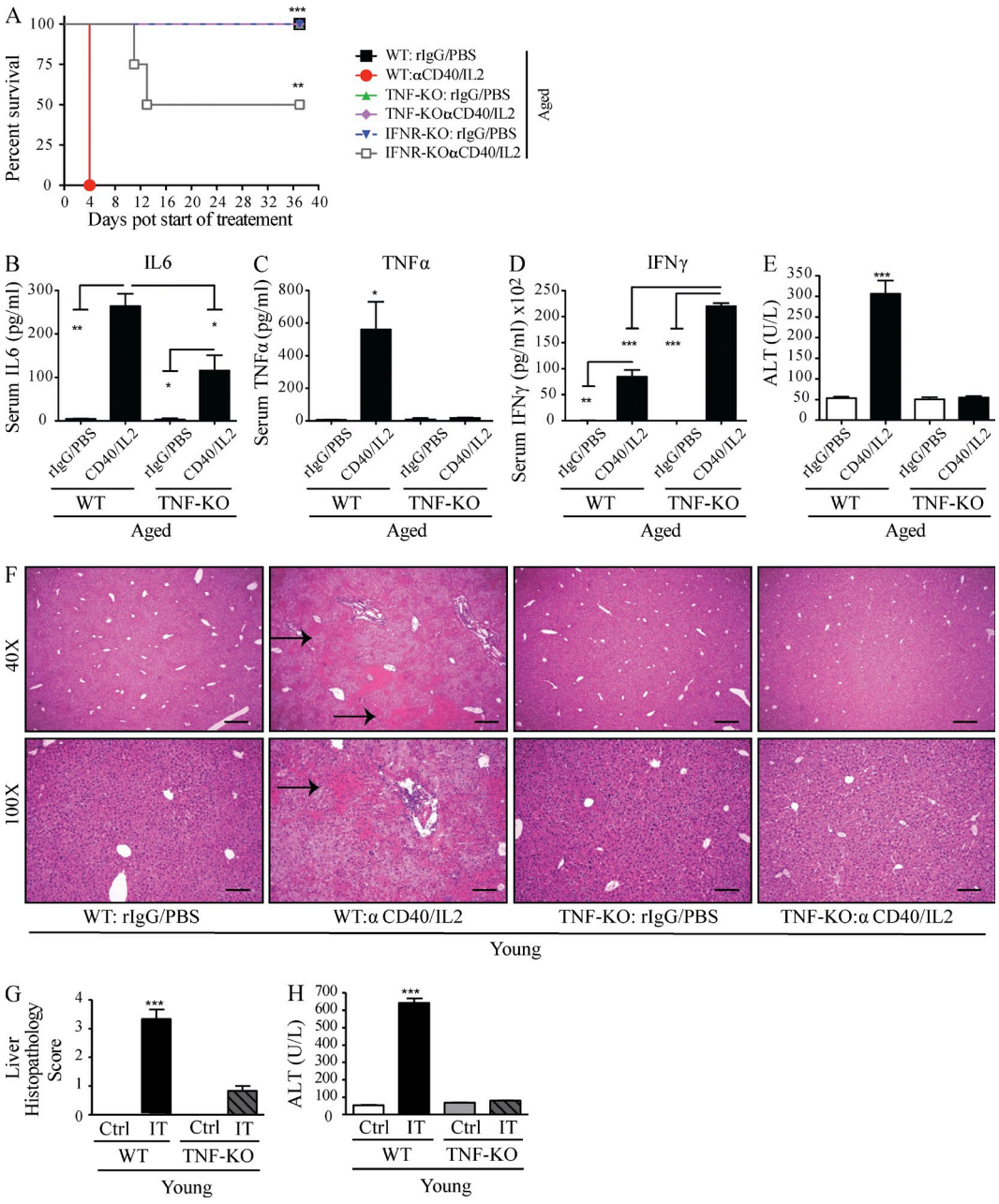

Figure 6. TNF-dependent systemic toxicity after low-dose anti-CD40/IL-2 treatment. (A) Survival of aged (16 mo) C57BL/6 (WT), IFNR-KO, and TNF-KO mice that received low-dose anti-CD40/IL-2 or aged matched controls, $n = 3$–5. Survival analysis was plotted according to the Kaplan-Meier method, and statistical differences were determined with the log-rank test. (B–E) Serum cytokines and ALT levels from the aged WT and age-matched TNF-KO (12 mo) including TNF, IL-6, and IFN-γ and ALT after 2 d of treatment, $n = 3$. (F–H) Young C57BL/6 WT and TNF-KO (2 mo) mice ($n = 3$) were treated for 2 d with high-dose anti-CD40/IL-2 or control treatment, and liver histopathology (F and G) and serum ALT (H) levels were assessed for each group. (F) Representative H&E liver images with black arrows pointing to areas of necrosis. Bars: (top) 500 µm; (bottom) 200 µm. Statistical analysis was by one-way ANOVA. ***, $P < 0.001$; **, $P < 0.01$; *, $P < 0.05$. Bar graphs represent the mean ± SEM. (A–H) are representative of two independent experiments.

levels were significantly decreased in aged-treated TNF-KO mice (Fig. 6 E). TNF-KO mice given IT demonstrated a significant decrease in hepatic necrosis (Fig. 6, F and G) and serum ALT (Fig. 6 H). These findings suggest that TNF plays a pivotal role in the induction of IT-mediated mortality and, in particular, liver damage.

TNF antagonist administration results in limited systemic toxicities, protection from liver pathology, and increased survival in aged mice after IT

Several TNF blockade therapies, including chimeric (i.e., Infliximab) and humanized monoclonal antibodies (i.e., Adalimumab) or a human TNF-R IgG 1 fusion protein (i.e., etanercept),

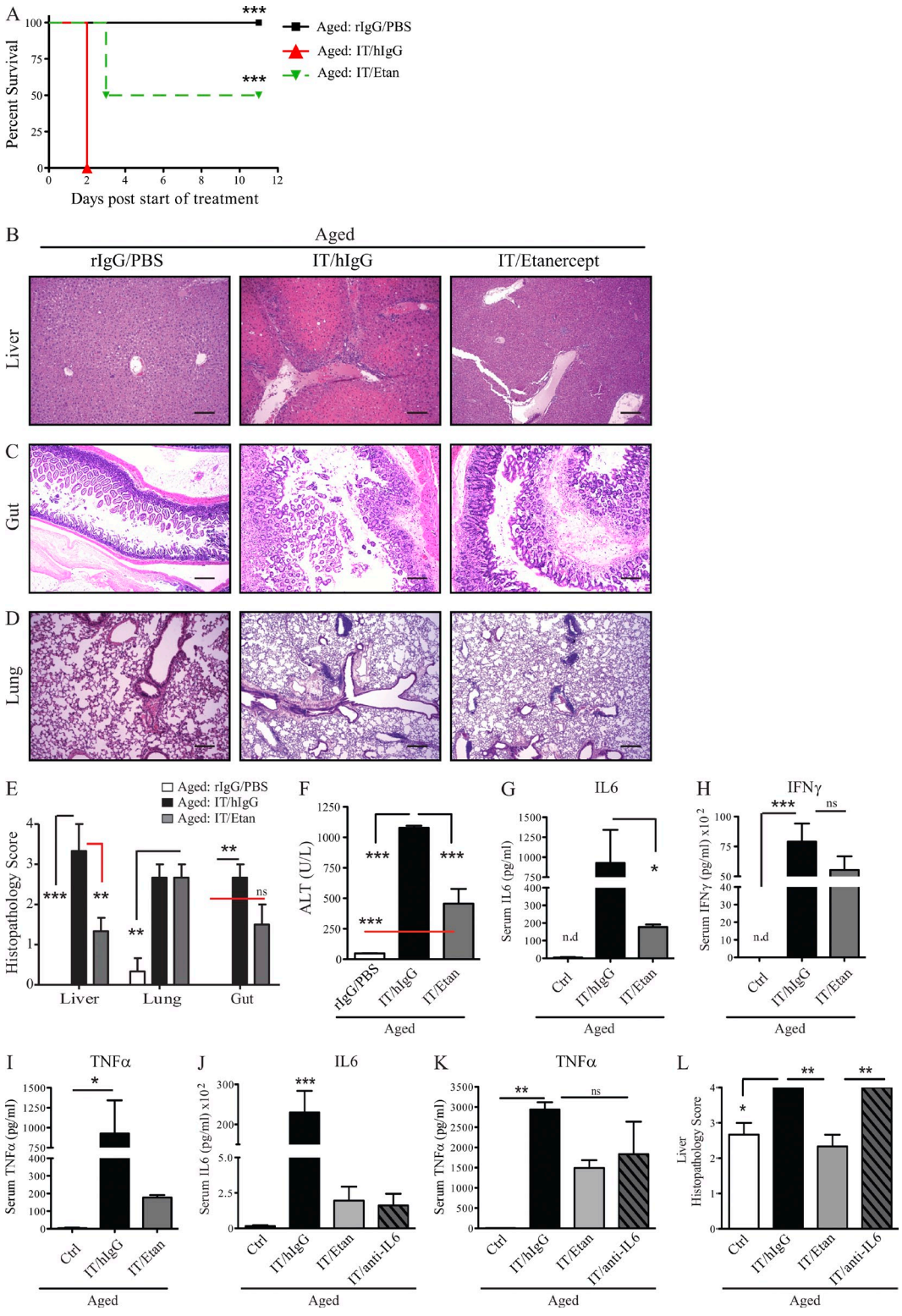

Figure 7. Combination of TNF blockade and anti-CD40/IL-2 increases survival, decreases systemic cytokine storm, and protects from liver pathology in aged mice. (A) Percent survival of aged (12 mo) C57BL/6 mice receiving low-dose anti-CD40/IL-2 with etanercept (Etan; 1.5 mg/0.2 ml s.c.), or hIgG (1.5 mg/0.2 ml s.c.) or rIgG/PBS, $n = 6–8$. Survival analysis was plotted according to the Kaplan-Meier method, and statistical differences were determined with the log-rank test. (B–F) Liver (B), gut (C), and lung (D) pathology and serum ALT (F) in aged mice (12 mo), $n = 3$. (B–D) One representative image from each group and each organ was captured. Bars, 50 µm. (E) Multiorgan histopathology score from B–D. (G–I) Serum cytokines from groups in B–F were examined for IL-6(G), IFN-γ (H), and TNF (I; day 2) in young (2 mo) and aged (12 mo) mice. Etanercept was administered on days −1 and 1.

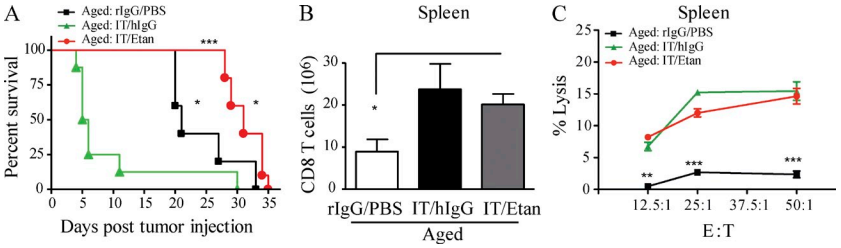

Figure 8. TNF blockade results in anti-tumor effects after anti-CD40/IL-2 therapy in aged mice. (A) Tumor survival in aged (12–15 mo) mice that received 3LL i.v. (day −3), followed by low-dose anti-CD40/IL-2 with etanercept (n = 8–10) or hIgG (n = 6) or PBS/rIgG (n = 6). (B and C) Number of $CD3^+$ $CD8^+$ T cells in the spleen after 9 d of treatment in aged (12 mo) C57BL/6 mice (B) and their percent lysis of total spleen cells against P815 tumors at different effector to target ratio (C), n = 3. Survival analysis was plotted according to the Kaplan-Meier method, and statistical differences were determined with the log-rank test. ***, P < 0.001, IT/hIgG versus IT/etanercept; *, P < 0.05, IT/Etanercept versus rIgG/PBS; *, P < 0.01, rIgG/PBS versus Low IT/hIgG. Survival curve of one of two independent experiments is represented. For B and C, values represent the mean ± SEM of one of two independent experiments tested by one-way or two-way ANOVA, respectively. ***, P < 0.001; **, P < 0.01; *, P < 0.05 compared with control group. A–C are representative of three independent experiments.

are successfully used for the clinical management of inflammation and to minimize autoimmune disorders such as rheumatoid arthritis, Crohn's disease, ulcerative colitis, psoriasis, and ankylosing spondylitis (Taylor and Feldmann, 2009; Taylor, 2010; Schett et al., 2011). Due to exciting results using TNF-KO mice, we were enthusiastic that TNF blockade for the amelioration of cytokine storm–induced toxicities in the aged may be readily translatable using preexisting, clinically approved treatment options. To test this hypothesis, we assessed the effects of TNF antagonists on IT-mediated toxicities using etanercept (Enbrel). Although etanercept contains a human TNF receptor, murine and human TNF share an 80% homology and etanercept has been shown to decrease TNF-mediated inflammation in mice (Grounds et al., 2005; Hodgetts et al., 2006; Hutchison et al., 2008; Surguladze et al., 2009; Nemoto et al., 2011). To test this hypothesis, aged mice were treated with etanercept, which resulted in significant increases in survival after anti-CD40/IL-2 IT. TNF blockade with IT allowed for greater survival, as 50% of aged mice survived the IT regimen when it was combined with TNF blockade (Fig. 7 A). This enhanced survival correlated with significant improvement in liver pathology (Fig. 7, B and E) in mice receiving combination treatment (IT/etanercept), which was concordant with decreases in serum ALT (Fig. 7 F). Interestingly, no differences were observed in the gut and lung pathology (Fig. 7, C–E), regardless of TNF blockade in the aged mice, further demonstrating the pivotal role of TNF in mediating hepatic changes in aged mice after IT and also demonstrating that the liver was the primary cause for mortality after IT. Interestingly, at the dose administered, etanercept only offered minimal protection in conjunction with the high-dose IT regimen (unpublished data).

In agreement with the TNF-KO data, serum cytokines were also affected after TNF blockade as IL-6 levels were diminished (Fig. 7 G). The induction of IFN-γ in aged mice was not inhibited by TNF blockade (Fig. 7 H). This may be important as it suggested that IFN-γ–dependent anti-tumor effects may still be preserved, as we have previously demonstrated that anti-tumor effects associated with anti-CD40/IL-2 in young mice are IFN-γ–dependent (Murphy et al., 2003). Moreover, serum TNF was diminished after etanercept but there were no significant differences in TNF production with or without TNF blockade (Fig. 7 I), as this drug only antagonizes mechanism of action of TNF.

Furthermore, we have noticed that TNF ablation using TNF-KO mice or etanercept led to marked reductions in IL-6 (Fig. 6 B and Fig. 7 G), suggesting that TNF may also mediate toxicity through modulation of IL-6 levels. To address this, we treated aged mice with IT with or without an IL-6 blocking antibody or with etanercept. Both TNF blockade and anti–IL-6 resulted in lower serum IL-6 and TNF (Fig. 7 K), yet that protection from liver pathology in aged mice was only observed when IT was combined with TNF blockade and not anti–IL-6 (Fig. 7 L). These data indicate that TNF blockade may be of use to ameliorate toxicities in aged tumor-bearing recipients after IT and possibly allow for anti-tumor effects to be maintained.

Increased survival in tumor-bearing aged mice using a TNF antagonist with IT

Because of TNF's contradictory roles in the suppression and promotion of tumor progression (Carswell et al., 1975; van Horssen et al., 2006; Calzascia et al., 2007; Sethi et al., 2008; Balkwill, 2009), it was imperative to determine whether IT-induced TNF, although critical to generation of systemic toxicities, may also be necessary for anti-tumor responses. Therefore, we next sought to ascertain if IT could be administered in aged tumor-bearing mice in combination with etanercept to prevent IT-associated mortality while preserving the anti-tumor effects induced by IT. Aged mice bearing the 3LL

(J–L) Aged C57BL/6 mice (12 mo old) received on day −1 either hIgG (1.5 mg/0.2 ml s.c.), or etanercept (Etan; 1.5 mg/0.2 ml s.c.), or anti–IL-6 antibody (1.0 mg/0.2ml i.p) with combination of low-dose anti-CD40/IL-2 (IT) on day 0. Control (Ctrl) group received rIgG/PBS, n = 3. (J and K) Serum cytokine levels for IL-6 (J) and TNF (K) were assessed after 2 d of treatment. (L) Liver histopathology from mice in J and K was assessed for each group. Values represent the mean ± SEM tested by one-way ANOVA with Bonferroni's post-tests. ***, P < 0.001; **, P < 0.01; *, P < 0.05 compared with control group. n.s: not significant. Data from A–I are representative of three independent experiments and data from J–L are representative of two independent experiments.

Lewis lung carcinoma were treated with anti-CD40/IL-2 IT and continuous etanercept administration. As observed earlier, aged tumor-bearing mice that received IT alone died very rapidly from acute toxicity compared with aged mice receiving tumor alone (Fig. 8 A). In contrast, aged tumor-bearing mice receiving continuous etanercept administration demonstrated 100% survival during an entire course of IT (12 d) and also resulted in significant anti-tumor effects with increased survival compared with mice receiving tumor alone (Fig. 8 A; death determined due to tumor upon necropsy, not depicted). This combination approach also resulted in CD8 T cell expansion in the spleens of aged mice (Fig. 8 B), as well as preservation of CD8 T cell lytic ability (Fig. 8 C) comparable to what was observed in young recipients (Murphy et al., 2003). These data indicate that TNF blockade allowed for aged tumor-bearing mice to receive effective IT resulting in increased survival, lessened toxicity, and preservation of anti-tumor responses.

DISCUSSION

Cancer IT has been shown to elicit successful anti-tumor responses both preclinically and clinically (Dougan and Dranoff, 2009). However, cytokine and antibody therapies can also lead to severe and systemic toxicities resulting in cessation of IT. Aging is associated with increased inflammation, potentially rendering cancer patients more susceptible to these toxicities. The mechanisms of increased "inflammaging" are not well understood and the majority of preclinical studies testing new immunotherapies have been investigated using young mouse models. Given that the mean age of a cancer patient is greater than 55 years old, these mouse models do not reflect the potential profound immune changes occurring that result in immune senescence and normal aging.

In the current study, we compared the effects of agonistic anti-CD40 and IL-2, as well as other immunostimulatory regimens, on systemic toxicities in young and aged mice. Our results demonstrate a pronounced age-dependent susceptibility to multiorgan toxicities after systemic immune stimulation resulting from a macrophage-mediated cytokine storm. We also show that aging results in increased inflammatory cytokine production leading to rapid mortality. Our data confirm that the fundamental process of inflammaging may serve as a predisposition to toxicities with age, indicating that application of systemic immune stimulation in the elderly must proceed with caution and demonstrating that increased susceptibility to toxicities from infectious agents may also result.

The rapid onset of mortality coupled with multiorgan tissue damage after IT in aged mice suggested that lethality may be associated with a systemic pathology similar to that experienced after sepsis or shock-like syndromes termed MODS (multiple organ dysfunction syndromes). Aged mice exhibited higher serum levels of proinflammatory cytokines, in particular TNF, IL-6, and IFN-γ, upon anti-CD40/IL-2 stimulation as well as after LPS treatment compared with young mice. We observed similar trends in organ pathology and serum liver enzymes in aged mice receiving IL-2/IL-12 IT as well. Although the aged mice did not succumb to IL-2/IL-12 treatments, they displayed (even at day 11 of therapy) increased systemic toxicities and multiorgan pathology as compared with young-treated mice. However, organ histopathology, although elevated in aged IL-2/IL-12 mice, was slightly lower than what was observed in aged mice treated with anti-CD40/IL-2, which could be indicative of the reasons that IL-2/IL-12–treated mice did not die. Additionally, we have also noted marked differences in histopathology on day 2 versus day 11 in young mice, and given that the mice treated with IL-2/IL-12 survived too and were analyzed for histopathology on day 11, the later time point may also contribute to the overt differences in pathology observed in IL-2/IL-12 mice. Overall, these data suggest that systemic toxicities are not anti-CD40/IL-2 specific but also occur with other cytokine therapies and with a different extent of fatality.

Given the plethora of recent data highlighting the role of microbiota in toxicity and disease (Arthur et al., 2012; Hooper et al., 2012; Gallimore and Godkin, 2013; Kamada et al., 2013), it begs the question as to the role of differential microbiota among institutional animal facilities in our studies. Importantly, in this study, given that the work presented here was performed across multiple organizations and across multiple strains of mice, all three (anti-CD40/IL-2, LPS, and IL-2/IL-12) immunomodulatory regimens resulted in similar patterns of toxicity and 100% mortality by day 2 of therapy (for anti-CD40/IL-2) in aged mice across all institutions. This suggests that the systemic toxicities observed in aged mice are independent on the animal housing conditions and any potential discrepancies that might arise from cleanliness of the animal facility or type of feed, all of which could affect intestinal microbiota.

The aged recipients not only produced higher levels of proinflammatory cytokines in circulation but also within the tissues where the damage was occurring. This was rapid, as death occurred within 2 d in aged mice. Interestingly, even mice as young as 9 mo succumbed to the toxicities. The lifespans of mouse and man are dramatically different. The average laboratory mouse lives 2–3 yr, whereas the average human lives ∼80 yr. As the vast majority of mouse cancer studies use mice starting at 2–3 mo of age, this would be roughly equivalent to treating an adolescent or young adult patient whose immune system is markedly different than an individual over the age of 55, the average age at which cancer is diagnosed and subsequently treated. Therefore, to more accurately reflect the typical cancer patient in the clinic, our data suggest that it may be more beneficial to perform preclinical studies in aged mice, particularly when attempting to accurately model toxicities.

In the immune cell depletion experiments, it was observed that whereas T cells are the predominant tumor effector cell, the systemic cytokine storm and mortality in aged mice were all dependent on macrophages. This age-associated dysregulation in macrophages was similar in humans, as it was observed that macrophages from both aged mice and humans exhibited heightened TNF and IL-6 production after LPS stimulation compared with macrophages from young mice or younger healthy donors.

The critical role for TNF is at least a partial mediator of these effects, as was demonstrated by the TNF-KO mice receiving IT exhibiting decreased serum IL-6, TNF, liver enzymes (ALT), and having preferential protection from liver pathology. In agreement with our data, mice deficient to either TNF or TNF receptors are less susceptible to endotoxic shock from high-dose LPS challenge and increased survival as opposed to WT mice (Smith et al., 1994; Paludan, 2000; Rosas et al., 2001; Kawa et al., 2010). Moreover, both liver enzymes and serum IL-6 were much lower after TNF blockade in our studies. This decrease in proinflammatory cytokines is likely a major contributor to the enhanced survival as well as diminished gastrointestinal and liver pathology. Although, IL-6 is well known as a hepatoprotective cytokine (Cressman et al., 1996), other studies have shown that long-term IL-6 exposure induced SOCS3 (suppressor of cytokine signaling 3) expression in hepatocytes, resulting in exacerbated liver injury (Senn et al., 2003; Rotter Sopasakis et al., 2004; Jin et al., 2006). Other reports have indicated that both IL-6 (Chen et al., 2009) and TNF (Korngold et al., 2003) mediate damage as a result of graft-versus-host disease (GVHD) after allogeneic hematopoietic stem cell transplantation. Interestingly, GVHD studies also suggest that different proinflammatory cytokines may play a more predominant role in a particular organ, although they may all contribute to the overall pathology. Our studies would support that TNF appears to be a primary mediator of hepatic damage after IT, whereas it is likely that other cytokines such as IL-6 may play a more predominant role in gut pathology. It is clear from these studies that liver failure is likely the principal cause of mortality after IT in aged mice.

The anti-tumor responses of anti-CD40/IL-2 are both CD8 T cell and IFN-γ mediated, as previously demonstrated (Murphy et al., 2003). In the current study, we have found that aged mice treated with anti-CD40/IL-2 and TNF blockade were able to mount effective anti-tumor responses against preexisting tumors. Not only did we see protection in the aged mice from IT-induced lethality, we also observed expansion of CD8 T cells and elevated IFN-γ levels using a lower dose of IT with etanercept and the induction of anti-tumor effects. The role of TNF in cancer is complex as it can both promote tumor progression and affect innate immune activation (Sethi et al., 2008). It is possible that the relatively short administration of TNF blockade during IT outweighs any tumor-promoting effects it can induce and the amelioration of toxicities allows for immune activation to manifest in anti-tumor effects.

Clinically, TNF blockade, in addition to being used to treat autoimmune diseases, is used as a treatment for immune-related adverse events (irAEs), particularly colitis, experienced after certain immunotherapeutic cancer regimens such as CTLA4 blockade (Minor et al., 2009). Therefore, there is precedent for its use during anti-cancer therapy. In these patients, however, treatment with the primary IT is halted due to irAE severity and anti-TNF therapy is administered afterward. Anti-tumor immunity is often maintained in these patients, further supporting the concept that TNF may not be essential to anti-tumor immunity and its blockade does not impede tumor immunity. In contrast to this clinical scenario, we show here that IT perhaps need not to be halted, but application of anti-TNF therapies (and in combination with inhibition of other cytokines such as IL-6) can be administered concurrently to alleviate toxicities while not adversely affecting anti-tumor responses.

It will be of particular interest to ascertain whether the increases of these proinflammatory cytokines associated with aging also occur after other cytoreductive insults such as chemotherapy and radiation therapy. Age, outside of frailty, may also play predisposing roles in other disease states, such as infectious disease, and toxicities, such as GVHD after allogeneic hematopoietic stem cell transplantation, due to the heightened proinflammatory state. Thus, aging strongly promotes inflammatory responses in both mouse and man, which can result in multiorgan pathologies after immune stimulation. This inflammatory sensitivity may predispose individuals after infection as well as cytoreductive cancer therapies to adverse events, but interventions affecting the cell types responsible (macrophages) or the inflammatory cytokines (TNF) themselves represent viable options. These studies underscore the importance of considering age as an important variable in the assessment of potential immunotherapies where the target population is predominantly aged.

MATERIALS AND METHODS

Mice

Female young (2–4 mo old), middle-aged (9–12 mo old), or aged (16–22 mo old) C57BL/6 or BALB/c mice were purchased from Charles River or from the animal production area at the National Cancer Institute. C57BL/6-TNF-KO young (4 mo old) or aged (16 mo old) mice, or C57BL/6–IFNR-KO aged mice (16 mo old) and their age-matched control WT-C57BL/6 were purchased from The Jackson Laboratory. Mice were housed in the animal facilities at the University of Nevada, Reno, the University of California, Davis, or the National Institute on Aging (NIA) at the National Institutes of Health under specific pathogen-free conditions. In each experiment, the young and aged mice were housed in the same animal facility. Animal studies were approved by the University of Nevada, Reno, the University of California, Davis, and the NIA, Baltimore campus Institutional Animal Care and Use committees.

Tumor cell lines

3LL Lewis lung carcinoma was purchased from the American Tissue Culture Collection. Cells were cultured in complete RF10 containing RPMI1640 medium supplemented with 10% FBS, 1% penicillin/streptomycin, 1% (2 mM) glutamine, 1% (1×) nonessential amino acids, 1% (1 mM) sodium pyruvate, 1.5% (15 mM) Hepes, and 1% (5×10^{-5} M) 2-mercaptoethanol at 37°C in a humidified atmosphere containing 5% CO_2. Cell viability was checked by trypan blue and counted with a hemocytometer. 3LL cells at 2.5×10^5 cells were suspended in 0.1 ml PBS and injected i.v. into young or aged C57BL/6 mice, and 3 d later IT was initiated.

Reagents

The agonistic anti–mouse CD40 antibody (clone FGK115B3) was generated via ascites production in our laboratory as previously described (Murphy et al., 2003). The endotoxin level of the anti-CD40 was <1 endotoxin unit/mg antibody as determined by a quantitative chromogenic limulus amebocyte lysate kit (Lonza). Recombinant human IL-2 (rhIL-2; TECIN Teceleukin; Roche) was provided by the National Cancer Institute (NCI). Recombinant mouse IL-12 (PeproTech) was purchased from commercial vendors. Etanercept (Amgen and Pfizer) was provided by E. Maverakis. Some mice received human or rat IgG (Jackson ImmunoResearch Laboratories, Inc.) as a control

for etanercept or anti-CD40 treatments, respectively. In some experiments, NK cells were depleted using 300 µg anti-NK1.1 (PK136) grown by the National Cell Culture Center. $CD8^+$ T cells were depleted using 500 µg of the rat antibody to mouse CD8 (clone YTS169.4) produced in ascites, and the endotoxin level was 3.6 EU/mg antibody. $CD4^+$ T cells were depleted with an anti-CD4 antibody at 500 µg (clone GK1.5; gift from G.B. Huffnagle, University of Michigan, Ann Arbor, MI). All antibodies were injected i.p., except etanercept which was injected subcutaneously.

Schedule of anti-CD40/IL-2 IT treatments

Mice were treated with agonist anti-CD40 antibody and rhIL-2 as previously described (Murphy et al., 2003). In brief, anti-CD40 was administered daily for a total of 5 consecutive days (day 0 to 4) and IL-2 was administered twice a day for a total of 4 d (days 1, 4, 8, and 11). Control mice received rat IgG (Jackson ImmunoResearch Laboratories, Inc.) and PBS (Cellgro). Survival was monitored daily. A high dose or low dose of anti-CD40/IL-2 was used and is described in figure legends and further specified below.

High-dose anti-CD40/IL-2. Mice received 80 µg of agonist anti-CD40 and 10^6 IU IL-2 in 0.2 ml PBS i.p. Control mice received 80 µg rIgG and PBS.

Low-dose anti-CD40/IL-2. Mice received 40 µg of agonist anti-CD40 and 2.5×10^5 IU IL-2 in 0.2 ml PBS i.p. Control mice received 40 µg rIgG and PBS.

TNF blockade with anti-CD40/IL-2. In some experiments in which TNF was blocked, etanercept was administered subcutaneously at 1.5 mg/0.2 ml PBS in aged mice. Etanercept was administered on days −1 and 1 for experiments when mice were scarified at day 2 of anti-CD40/IL-2 therapy. In survival from systemic toxicities and anti-tumor studies, etanercept was administered on days −1, 1, 3, 7, and 9. Tumor cells were injected i.v. on day −3 with day 0 being the start of anti-CD40/IL-2 treatment.

IL-6 blockade with anti-CD40/IL-2. To block IL-6, aged mice received a rat monoclonal antibody (CNTO 345) specific for mouse IL-6 (Centocor Research and Development Inc.) at 1.0 mg/0.2 ml in PBS on day −1 before the start of anti-CD40/IL-2 IT treatment on day 0. Mice were scarified at day 2 of IT for serum cytokine measurements and liver pathology.

Schedule of pulse IL-2/IL-12 treatments

Recombinant mouse IL-12 at 0.5 µg/0.2 ml was administered to BALB/c mice i.p for 5 consecutive days (says 0 to 4) during week 1 and for another 4 consecutive days during week 2 of IT (days 7 to 11). RhIL-2 at 3×10^5 IU/0.2 ml was administered i.p twice a day, on days 0, 4, and 7.

Macrophage depletion in vivo

Macrophages were depleted in vivo using LC (Encapsula Nano Sciences) and administered on days −2 and 0 for experiments requiring euthanasia on day 2 or on days −2, 0, 2, and 4 for survival studies. Day 0 is the start of anti-CD40/IL-2 treatment, which is descried in the above section for the schedule of anti-CD40/IL-2 therapy. Clodronate or control-loaded liposomes were injected at 0.2 ml per dose i.p. 95% of macrophages were depleted and this was verified by staining for flow cytometry for $CD45^+$ (Pacific blue), $CD19^-$ (PE), $CD11b^+$ (APC-Cy7), and $F4/80^+$ (APC) cells in the spleen and peritoneal lavage.

LPS treatment in vivo

Young, middle-aged, or aged C57BL/6 mice received a single 0.2 ml i.p injection of either PBS or LPS derived from *Escherichia coli* serotype 055:B5 (Sigma-Aldrich) resuspended in PBS at doses between 1.5 mg/kg body mass. Mice were examined continuously for survival experiments.

Human and murine macrophage studies

PBMCs were collected from healthy young or aged donors with written informed consent in accordance with the IRB-approved human subject protocol #2003054 of the Clinical Research Branch, National Institute on Aging. PBMCs from aged subjects were also collected from participants in the National Institute on Aging Baltimore Longitudinal Study of Aging (BLSA), approved by the IRB, and all participants signed informed consent. Details of the BLSA recruitment and testing methodology are described elsewhere (Shock et al., 1984). Human PBMCs were obtained by Ficoll-Hypaque density centrifugation after which monocytes were purified from PBMCs using the human Monocyte Isolation kit II (Miltenyi Biotec). Isolated monocytes were typically >94% after isolation. Monocytes were either directly cultured in AIM-V serum-free media (Invitrogen) on poly:IC-coated plates and stimulated with 50 ng/ml human recombinant macrophage CSF (hM-CSF; GenScript USA Inc.) for 6 d, washed, and recultured in AIM-V with hM-CSF and 0.5% participant plasma for an additional 3–4 d. The purity of the cultured human macrophage generated was >92% based on flow cytometric analysis and/or Giemsa/nonspecific esterase staining. Macrophages isolated from these cultures were harvested using TrypLE Express Stable Trypsin-Like Enzyme with Phenol red (Life Technologies) and gently scraping with a rubber policeman. Cells were washed and plated on poly:IC-coated plates and stimulated with 50 ng/ml LPS for 48 h, and then the supernatants were collected to evaluate cytokine expression.

Murine BMDMs were isolated from the femurs of young and aged C57BL/6 mice as previously described (Zhang et al., 2008). BM cells were suspended, counted, and cultured on tissue culture plates precoated with poly:IC using a BM culture media containing DMEM (Invitrogen), 10% heat-inactivated fetal calf serum, 2 Mm L-glutamine, 100 U/ml penicillin, 100 ng/ml streptomycin, 20% L929 (American Type Culture Collection no. CCL-1)–conditioned medium, and 100 ng/ml hM-CSF for 6 d at 37°C in 10% CO_2. In certain experiments, BM cells were enriched for murine monocytes before culture using EasySep Mouse Monocyte Enrichment kit (STEMCELL Technologies). After 6–7 d, macrophages were removed by treatment with TrypLE Express Stable Trypsin-Like Enzyme with Phenol red and gently scraping with a rubber policemen. The cells were isolated, cultured, and stimulated with 50 ng/ml LPS for 24 h, and then the supernatants were collected to evaluate cytokine expression. Macrophage purity was found to be >94% live macrophages as assessed by staining with anti–CD11b-PE and anti–F4/80-FITC (BD).

Serum cytokine quantification

Serum levels of TNF, IFN-γ, and IL-6 were quantified by multiplex measurement using the Cytometric Bead Array CBA (BD) kit according to manufacturer's instructions. Each sample was run in triplicate. Upon analysis of raw data, the MFIs in the detection reagent channel of each bead cluster were quantified. Serum cytokine concentrations were then extrapolated relative to a standard curve created by serial dilution of multiplexed mouse standard cytokines run in parallel. Data were acquired on a Fortessa cell analyzer using FACSDiva software (BD) and analyzed using FlowJo software (Tree Star). Standard regressions and sample statistical significance was determined using Prism data analysis software (GraphPad Software).

Supernatant cytokine determinations

For certain studies, human and murine cytokines were analyzed in culture supernatants using Bio-Plex Mouse and Human Cytokine Singleplex kits according to the manufacturer's instructions (Bio-Rad Laboratories).

Colorimetric liver enzyme assay

The concentration (units per liter) of serum ALT in blood was quantified using the ALT Enzymatic Assay kit (ID Labs, Inc.) according to manufacturer instructions. Colorimetric determination of ALT levels was performed by reading of absorbance of each well at 340 nm on a VERSAmax Tunable Plate Reader (Molecular Devices) and data were collected using SOFTmax PRO software (Molecular Devices). Dilutions of the pyruvate control, included in the kit, were used to construct a standard curve to calibrate the assay. Serum samples were assayed in triplicate.

Histopathology and grading score

Liver, lung, and whole intestines were collected on day 2 of IT, flushed and fixed in 10% paraformaldehyde, embedded in paraffin, cut in sections, and

stained with hematoxylin and eosin (H&E). All tissues were prepared and stained at the Histology Consultation Services, Inc. in Everson, WA. Images were captured with a BX4 microscope (Olympus) equipped with a Q-color3 camera and 10× numerical aperture objective lens. Magnification for each captured image is specified for each experiment in the figure legend. Grading of histopathological inflammation was performed using a grading scale from 0 to 4 in a blind fashion by a board-certified pathologist. Grading score criteria of tissue inflammation and necrosis ranged from 0 to 4, with 0 = no inflammation, 1 = minimal/intermediate, 2 = mild, 3 = moderate, and 4 = severe with tissue necrosis. This grading score for liver, lung, and gastrointestinal tract was consistent with the previously published grading systems (Yousem et al., 1996; Anonymous, 1997).

RNA isolation and cDNA synthesis

Total RNA from mouse tissues was isolated using RNeasy mini kit (QIAGEN). RNA quantities were standardized across samples with a maximum of 1 µg of total RNA reverse transcribed using a high capacity cDNA reverse transcription kit (Applied Biosystems) containing RT buffer, a random primer, reverse transcription, and RNase inhibitor. RNA was transcribed for 60 min at 37°C, for 5 min at 95°C, and then for 5 min at 4°C using AB Veriti Therma Cyler (Applied Biosystems) with 96-well Aluminum Sample Block Module.

Real-time PCR

Quantitative real-time PCR was performed using AB Step-ONE Plus (Applied Biosystems) in the presence of SYBR Green Supermix (Applied Biosystems). Primer assays for TNF, IFN-γ, and IL-6 were purchased from QIAGEN. mRNA levels were calculated using the comparative threshold cycle method (C_t). C_t values for the housekeeping gene (GAPDH) and for the genes of interest were determined, and the difference between the C_t values of each gene of interest and the mean GAPDH Ct was calculated (ΔC_t). Differences in ΔC_t ($\Delta\Delta C_t$) of genes of interest in treatment groups (anti-CD40/IL-2) were normalized to control groups (rIgG/PBS) as shown in the following equation: $\Delta\Delta C_t = \Delta C_t(\text{sample}) - \Delta C_t(\text{mean of control group})$. RT-PCR data are presented as fold change expression = $2^{-\Delta\Delta Ct}$ of each cytokine in comparison to control groups (rIgG/PBS).

Flow cytometry

10^6 cells from single cell suspensions from spleen or peritoneal lavage were first incubated with Fc block (BD) and then labeled with anti–mouse antibodies, including FITC anti–mouse CD3 (clone 145-2C11), AF700 anti–mouse CD8 (clone 53–6.7), Pacific blue anti–mouse CD45 (clone 30-F11), APC anti–mouse F4/80 (clone BM8), APC rIgG2a (clone RTK2758), APC-Cy7 anti–mouse CD11b (clone M1/70), and PE anti–mouse CD19 (clone 1D3). Anti–mouse CD19 was purchased from BD. All other antibodies were purchased from BioLegend. Listmode data files were collected using a Fortessa cell analyzer with FACSDiva software (BD). All datasets were analyzed using FlowJo software.

Antibody-redirected lysis assay

Splenic $CD8^+$ T cells (effectors) from aged mice treated with RIgG/PBS or anti-CD40/IL-2 or anti-CD40/IL-2/Etanercept for 9 d were serially diluted in a 96-well U-bottom plates in RF10c media as previously described (Tietze et al., 2012). P815 cells (targets) were labeled with 100 µCi ^{51}Cr (NEZ030S; Perkin Elmer) per 10^6 cells and incubated for 30 min with 1 µg/ml anti-CD3e (eBioscience; clone HIT3a). 10^4 P815 targets were added to each well at different effector to target (E:T) ratio and incubated at 37°C for 4 h. Supernatants were removed, mixed 1:1 with scintillation fluid, and analyzed on a scintillation counter (Wallac). Maximum release was determined by adding 100 µl 1× Triton X-100 detergent (Sigma-Aldrich) to target cells. Spontaneous release was determined by adding 100 µl RF10c media to 100 µl of target cells. Specific ^{51}Cr release was calculated as: % lysis = 100% × (experimental − spontaneous)/(maximum − spontaneous).

Statistical analysis

Statistical analysis was performed using Prism software. Data were expressed as mean ± SEM. For analysis of three or more groups, the nonparametric ANOVA test was performed with Bonferroni's post-test. Analysis of differences between two normally distributed test groups was performed using the Student's *t* test. Welch's correction was applied to Student's *t* test datasets with significant differences in variance.

We thank Monja Metcalf and Weihong Ma for technical help.

This work was supported by grants from the National Institutes of Health (CA0905572 and AG034874) and by the Intramural Research Program of the National Institute on Aging, National Institutes of Health.

The authors declare no competing financial interests.

Submitted: 10 June 2013
Accepted: 5 September 2013

REFERENCES

Aggarwal, B.B. 2003. Signalling pathways of the TNF superfamily: a double-edged sword. *Nat. Rev. Immunol.* 3:745–756. http://dx.doi.org/10.1038/nri1184

Anonymous. 1997. Banff schema for grading liver allograft rejection: an international consensus document. *Hepatology*. 25:658–663. http://dx.doi.org/10.1002/hep.510250328

Arthur, J.C., E. Perez-Chanona, M. Mühlbauer, S. Tomkovich, J.M. Uronis, T.J. Fan, B.J. Campbell, T. Abujamel, B. Dogan, A.B. Rogers, et al. 2012. Intestinal inflammation targets cancer-inducing activity of the microbiota. *Science*. 338:120–123. http://dx.doi.org/10.1126/science.1224820

Attarwala, H. 2010. TGN1412: From Discovery to Disaster. *J Young Pharm*. 2:332–336. http://dx.doi.org/10.4103/0975-1483.66810

Balkwill, F. 2009. Tumour necrosis factor and cancer. *Nat. Rev. Cancer*. 9: 361–371. http://dx.doi.org/10.1038/nrc2628

Berger, C., M. Berger, R.C. Hackman, M. Gough, C. Elliott, M.C. Jensen, and S.R. Riddell. 2009. Safety and immunologic effects of IL-15 administration in nonhuman primates. *Blood*. 114:2417–2426. http://dx.doi.org/10.1182/blood-2008-12-189266

Blay, J.Y., S. Negrier, V. Combaret, S. Attali, E. Goillot, Y. Merrouche, A. Mercatello, A. Ravault, J.M. Tourani, J.F. Moskovtchenko, et al. 1992. Serum level of interleukin 6 as a prognosis factor in metastatic renal cell carcinoma. *Cancer Res.* 52:3317–3322.

Boccoli, G., R. Masciulli, E.M. Ruggeri, P. Carlini, G. Giannella, E. Montesoro, G. Mastroberardino, G. Isacchi, U. Testa, F. Calabresi, et al. 1990. Adoptive immunotherapy of human cancer: the cytokine cascade and monocyte activation following high-dose interleukin 2 bolus treatment. *Cancer Res.* 50:5795–5800.

Boparai, M.K., and B. Korc-Grodzicki. 2011. Prescribing for older adults. *Mt. Sinai J. Med*. 78:613–626. http://dx.doi.org/10.1002/msj.20278

Brüünsgaard, H., and B.K. Pedersen. 2003. Age-related inflammatory cytokines and disease. *Immunol. Allergy Clin. North Am*. 23:15–39. http://dx.doi.org/10.1016/S0889-8561(02)00056-5

Calzascia, T., M. Pellegrini, H. Hall, L. Sabbagh, N. Ono, A.R. Elford, T.W. Mak, and P.S. Ohashi. 2007. TNF-alpha is critical for antitumor but not antiviral T cell immunity in mice. *J. Clin. Invest*. 117:3833–3845.

Carswell, E.A., L.J. Old, R.L. Kassel, S. Green, N. Fiore, and B. Williamson. 1975. An endotoxin-induced serum factor that causes necrosis of tumors. *Proc. Natl. Acad. Sci. USA*. 72:3666–3670. http://dx.doi.org/10.1073/pnas.72.9.3666

Chen, X., R. Das, R. Komorowski, A. Beres, M.J. Hessner, M. Mihara, and W.R. Drobyski. 2009. Blockade of interleukin-6 signaling augments regulatory T-cell reconstitution and attenuates the severity of graft-versus-host disease. *Blood*. 114:891–900. http://dx.doi.org/10.1182/blood-2009-01-197178

Chung, H.Y., M. Cesari, S. Anton, E. Marzetti, S. Giovannini, A.Y. Seo, C. Carter, B.P. Yu, and C. Leeuwenburgh. 2009. Molecular inflammation: underpinnings of aging and age-related diseases. *Ageing Res. Rev.* 8:18–30. http://dx.doi.org/10.1016/j.arr.2008.07.002

Cressman, D.E., L.E. Greenbaum, R.A. DeAngelis, G. Ciliberto, E.E. Furth, V. Poli, and R. Taub. 1996. Liver failure and defective hepatocyte regeneration in interleukin-6-deficient mice. *Science*. 274:1379–1383. http://dx.doi.org/10.1126/science.274.5291.1379

Di Giacomo, A.M., M. Biagioli, and M. Maio. 2010. The emerging toxicity profiles of anti-CTLA-4 antibodies across clinical indications. *Semin.*

Oncol. 37:499–507. http://dx.doi.org/10.1053/j.seminoncol.2010.09.007

Dougan, M., and G. Dranoff. 2009. Immune therapy for cancer. *Annu. Rev. Immunol.* 27:83–117. http://dx.doi.org/10.1146/annurev.immunol.021908.132544

Ferrucci, L., A. Corsi, F. Lauretani, S. Bandinelli, B. Bartali, D.D. Taub, J.M. Guralnik, and D.L. Longo. 2005. The origins of age-related proinflammatory state. *Blood*. 105:2294–2299. http://dx.doi.org/10.1182/blood-2004-07-2599

Franceschi, C. 2007. Inflammaging as a major characteristic of old people: can it be prevented or cured? *Nutr. Rev.* 65:S173–S176. http://dx.doi.org/10.1301/nr.2007.dec.S173-S176

Franceschi, C., M. Bonafè, S. Valensin, F. Olivieri, M. De Luca, E. Ottaviani, and G. De Benedictis. 2000. Inflamm-aging. An evolutionary perspective on immunosenescence. *Ann. N. Y. Acad. Sci.* 908:244–254. http://dx.doi.org/10.1111/j.1749-6632.2000.tb06651.x

Gallimore, A.M., and A. Godkin. 2013. Epithelial barriers, microbiota, and colorectal cancer. *N. Engl. J. Med.* 368:282–284. http://dx.doi.org/10.1056/NEJMcibr1212341

Gantner, F., M. Leist, A.W. Lohse, P.G. Germann, and G. Tiegs. 1995. Concanavalin A-induced T-cell-mediated hepatic injury in mice: the role of tumor necrosis factor. *Hepatology*. 21:190–198.

Grounds, M.D., M. Davies, J. Torrisi, T. Shavlakadze, J. White, and S. Hodgetts. 2005. Silencing TNFalpha activity by using Remicade or Enbrel blocks inflammation in whole muscle grafts: an in vivo bioassay to assess the efficacy of anti-cytokine drugs in mice. *Cell Tissue Res.* 320:509–515. http://dx.doi.org/10.1007/s00441-005-1102-z

Hack, C.E., E.R. De Groot, R.J. Felt-Bersma, J.H. Nuijens, R.J. Strack Van Schijndel, A.J. Eerenberg-Belmer, L.G. Thijs, and L.A. Aarden. 1989. Increased plasma levels of interleukin-6 in sepsis. *Blood*. 74:1704–1710.

Hodgetts, S., H. Radley, M. Davies, and M.D. Grounds. 2006. Reduced necrosis of dystrophic muscle by depletion of host neutrophils, or blocking TNFalpha function with Etanercept in mdx mice. *Neuromuscul. Disord.* 16:591–602. http://dx.doi.org/10.1016/j.nmd.2006.06.011

Hooper, L.V., D.R. Littman, and A.J. Macpherson. 2012. Interactions between the microbiota and the immune system. *Science*. 336:1268–1273. http://dx.doi.org/10.1126/science.1223490

Hutchison, S., B.S. Choo-Kang, R.V. Bundick, A.J. Leishman, J.M. Brewer, I.B. McInnes, and P. Garside. 2008. Tumour necrosis factor-alpha blockade suppresses murine allergic airways inflammation. *Clin. Exp. Immunol.* 151:114–122. http://dx.doi.org/10.1111/j.1365-2249.2007.03509.x

Jin, X., T.A. Zimmers, E.A. Perez, R.H. Pierce, Z. Zhang, and L.G. Koniaris. 2006. Paradoxical effects of short- and long-term interleukin-6 exposure on liver injury and repair. *Hepatology*. 43:474–484. http://dx.doi.org/10.1002/hep.21087

Kamada, N., S.U. Seo, G.Y. Chen, and G. Núñez. 2013. Role of the gut microbiota in immunity and inflammatory disease. *Nat. Rev. Immunol.* 13:321–335. http://dx.doi.org/10.1038/nri3430

Kawa, K., H. Tsutsui, R. Uchiyama, J. Kato, K. Matsui, Y. Iwakura, T. Matsumoto, and K. Nakanishi. 2010. IFN-gamma is a master regulator of endotoxin shock syndrome in mice primed with heat-killed Propionibacterium acnes. *Int. Immunol.* 22:157–166. http://dx.doi.org/10.1093/intimm/dxp122

Korngold, R., J.C. Marini, M.E. de Baca, G.F. Murphy, and J. Giles-Komar. 2003. Role of tumor necrosis factor-alpha in graft-versus-host disease and graft-versus-leukemia responses. *Biol. Blood Marrow Transplant.* 9:292–303. http://dx.doi.org/10.1016/S1083-8791(03)00087-9

Krüttgen, A., and S. Rose-John. 2012. Interleukin-6 in sepsis and capillary leakage syndrome. *J. Interferon Cytokine Res.* 32:60–65. http://dx.doi.org/10.1089/jir.2011.0062

Leon, L.R., A.A. White, and M.J. Kluger. 1998. Role of IL-6 and TNF in thermoregulation and survival during sepsis in mice. *Am. J. Physiol.* 275:R269–R277.

McInnes, I.B., B.P. Leung, R.D. Sturrock, M. Field, and F.Y. Liew. 1997. Interleukin-15 mediates T cell-dependent regulation of tumor necrosis factor-alpha production in rheumatoid arthritis. *Nat. Med.* 3:189–195. http://dx.doi.org/10.1038/nm0297-189

Minor, D.R., K. Chin, and M. Kashani-Sabet. 2009. Infliximab in the treatment of anti-CTLA4 antibody (ipilimumab) induced immune-related colitis. *Cancer Biother. Radiopharm.* 24:321–325. http://dx.doi.org/10.1089/cbr.2008.0607

Munford, R.S. 2006. Severe sepsis and septic shock: the role of gram-negative bacteremia. *Annu. Rev. Pathol.* 1:467–496. http://dx.doi.org/10.1146/annurev.pathol.1.110304.100200

Murphy, W.J., L. Welniak, T. Back, J. Hixon, J. Subleski, N. Seki, J.M. Wigginton, S.E. Wilson, B.R. Blazar, A.M. Malyguine, et al. 2003. Synergistic anti-tumor responses after administration of agonistic antibodies to CD40 and IL-2: coordination of dendritic and CD8+ cell responses. *J. Immunol.* 170:2727–2733.

Nemoto, H., S. Konno, H. Sugimoto, H. Nakazora, N. Nomoto, M. Murata, H. Kitazono, and T. Fujioka. 2011. Anti-TNF therapy using etanercept suppresses degenerative and inflammatory changes in skeletal muscle of older SJL/J mice. *Exp. Mol. Pathol.* 90:264–270. http://dx.doi.org/10.1016/j.yexmp.2011.02.003

Paludan, S.R. 2000. Synergistic action of pro-inflammatory agents: cellular and molecular aspects. *J. Leukoc. Biol.* 67:18–25.

Repetto, L., and L. Balducci. 2002. A case for geriatric oncology. *Lancet Oncol.* 3:289–297. http://dx.doi.org/10.1016/S1470-2045(02)00730-1

Rosas, G.O., S.J. Zieman, M. Donabedian, K. Vandegaer, and J.M. Hare. 2001. Augmented age-associated innate immune responses contribute to negative inotropic and lusitropic effects of lipopolysaccharide and interferon gamma. *J. Mol. Cell. Cardiol.* 33:1849–1859. http://dx.doi.org/10.1006/jmcc.2001.1448

Rotter Sopasakis, V., B.M. Larsson, A. Johansson, A. Holmäng, and U. Smith. 2004. Short-term infusion of interleukin-6 does not induce insulin resistance in vivo or impair insulin signalling in rats. *Diabetologia*. 47:1879–1887. http://dx.doi.org/10.1007/s00125-004-1544-y

Schett, G., L.C. Coates, Z.R. Ash, S. Finzel, and P.G. Conaghan. 2011. Structural damage in rheumatoid arthritis, psoriatic arthritis, and ankylosing spondylitis: traditional views, novel insights gained from TNF blockade, and concepts for the future. *Arthritis Res. Ther.* 13:S4. http://dx.doi.org/10.1186/ar3417

Senn, J.J., P.J. Klover, I.A. Nowak, T.A. Zimmers, L.G. Koniaris, R.W. Furlanetto, and R.A. Mooney. 2003. Suppressor of cytokine signaling-3 (SOCS-3), a potential mediator of interleukin-6-dependent insulin resistance in hepatocytes. *J. Biol. Chem.* 278:13740–13746. http://dx.doi.org/10.1074/jbc.M210689200

Sethi, G., B. Sung, and B.B. Aggarwal. 2008. TNF: a master switch for inflammation to cancer. *Front. Biosci.* 13:5094–5107. http://dx.doi.org/10.2741/3066

Shalaby, M.R., A. Waage, L. Aarden, and T. Espevik. 1989. Endotoxin, tumor necrosis factor-alpha and interleukin 1 induce interleukin 6 production in vivo. *Clin. Immunol. Immunopathol.* 53:488–498. http://dx.doi.org/10.1016/0090-1229(89)90010-X

Sheron, N., J.N. Lau, J. Hofmann, R. Williams, and G.J. Alexander. 1990. Dose-dependent increase in plasma interleukin-6 after recombinant tumour necrosis factor infusion in humans. *Clin. Exp. Immunol.* 82:427–428. http://dx.doi.org/10.1111/j.1365-2249.1990.tb05465.x

Shock, N.W., R.C. Greulich, R. Andres, D. Arenberg, P.T. Costa Jr., E.G. Lakatta, and J.D. Tobin. 1984. Normal Human Aging: The Baltimore Longitudinal Study of Aging. U.S. Government Printing Office, Washington, DC. 661 pp.

Smith, S.R., C. Terminelli, L. Kenworthy-Bott, A. Calzetta, and J. Donkin. 1994. The cooperative effects of TNF-alpha and IFN-gamma are determining factors in the ability of IL-10 to protect mice from lethal endotoxemia. *J. Leukoc. Biol.* 55:711–718.

Suntharalingam, G., M.R. Perry, S. Ward, S.J. Brett, A. Castello-Cortes, M.D. Brunner, and N. Panoskaltsis. 2006. Cytokine storm in a phase 1 trial of the anti-CD28 monoclonal antibody TGN1412. *N. Engl. J. Med.* 355:1018–1028. http://dx.doi.org/10.1056/NEJMoa063842

Surguladze, D., D. Deevi, N. Claros, E. Corcoran, S. Wang, M.J. Plym, Y. Wu, J. Doody, D.J. Mauro, L. Witte, et al. 2009. Tumor necrosis factor-alpha and interleukin-1 antagonists alleviate inflammatory skin changes associated with epidermal growth factor receptor antibody therapy in mice. *Cancer Res.* 69:5643–5647. http://dx.doi.org/10.1158/0008-5472.CAN-09-0487

Taylor, P.C. 2010. Pharmacology of TNF blockade in rheumatoid arthritis and other chronic inflammatory diseases. *Curr. Opin. Pharmacol.* 10:308–315. http://dx.doi.org/10.1016/j.coph.2010.01.005

Taylor, P.C., and M. Feldmann. 2009. Anti-TNF biologic agents: still the therapy of choice for rheumatoid arthritis. *Nat Rev Rheumatol.* 5:578–582. http://dx.doi.org/10.1038/nrrheum.2009.181

Tietze, J.K., D.E. Wilkins, G.D. Sckisel, M.N. Bouchlaka, K.L. Alderson, J.M. Weiss, E. Ames, K.W. Bruhn, N. Craft, R.H. Wiltrout, et al. 2012. Delineation of antigen-specific and antigen-nonspecific CD8(+) memory T-cell responses after cytokine-based cancer immunotherapy. *Blood.* 119:3073–3083. http://dx.doi.org/10.1182/blood-2011-07-369736

van Horssen, R., T.L. Ten Hagen, and A.M. Eggermont. 2006. TNF-alpha in cancer treatment: molecular insights, antitumor effects, and clinical utility. *Oncologist.* 11:397–408. http://dx.doi.org/10.1634/theoncologist.11-4-397

Vonderheide, R.H., K.T. Flaherty, M. Khalil, M.S. Stumacher, D.L. Bajor, N.A. Hutnick, P. Sullivan, J.J. Mahany, M. Gallagher, A. Kramer, et al. 2007. Clinical activity and immune modulation in cancer patients treated with CP-870,893, a novel CD40 agonist monoclonal antibody. *J. Clin. Oncol.* 25:876–883. http://dx.doi.org/10.1200/JCO.2006.08.3311

Waldmann, T.A. 2006. The biology of interleukin-2 and interleukin-15: implications for cancer therapy and vaccine design. *Nat. Rev. Immunol.* 6:595–601. http://dx.doi.org/10.1038/nri1901

Weber, J.S., K.C. Kähler, and A. Hauschild. 2012. Management of immune-related adverse events and kinetics of response with ipilimumab. *J. Clin. Oncol.* 30:2691–2697. http://dx.doi.org/10.1200/JCO.2012.41.6750

Wigginton, J.M., K.L. Komschlies, T.C. Back, J.L. Franco, M.J. Brunda, and R.H. Wiltrout. 1996. Administration of interleukin 12 with pulse interleukin 2 and the rapid and complete eradication of murine renal carcinoma. *J. Natl. Cancer Inst.* 88:38–43. http://dx.doi.org/10.1093/jnci/88.1.38

Wigginton, J.M., E. Gruys, L. Geiselhart, J. Subleski, K.L. Komschlies, J.W. Park, T.A. Wiltrout, K. Nagashima, T.C. Back, and R.H. Wiltrout. 2001. IFN-gamma and Fas/FasL are required for the antitumor and antiangiogenic effects of IL-12/pulse IL-2 therapy. *J. Clin. Invest.* 108:51–62.

Yousem, S.A., G.J. Berry, P.T. Cagle, D. Chamberlain, A.N. Husain, R.H. Hruban, A. Marchevsky, N.P. Ohori, J. Ritter, S. Stewart, and H.D. Tazelaar. 1996. Revision of the 1990 working formulation for the classification of pulmonary allograft rejection: Lung Rejection Study Group. *J. Heart Lung Transplant.* 15:1–15.

Zhang, X., R. Goncalves, and D.M. Mosser. 2008. The isolation and characterization of murine macrophages. *Curr. Protoc. Immunol.* Chapter 14:1. http://dx.doi.org/10.1002/0471142735.im1401s83